

The Entropy-Driven X-ray Evolution of Galaxy Clusters

Richard G. Bower,¹

¹ *Dept. of Physics, University of Durham, South Road, Durham, DH1 3LE, U. K. (e-mail: R.G.Bower@durham.ac.uk)*

ABSTRACT

Observations of the evolution of the galaxy cluster X-ray luminosity function suggest that the entropy of the intra-cluster medium plays a significant role in determining the development of cluster X-ray properties. I present a theoretical framework in which the evolution of the entropy of the central intra-cluster gas is explicitly taken into account. The aim of this work is to develop a theoretical context within which steadily improving measurements of the X-ray luminosities and temperatures of distant galaxy clusters can be interpreted. I discuss the possible range of entropy evolution parameters and relate these to the physical processes heating and cooling the intra-cluster medium. The practical application of this work is demonstrated by combining currently available evolutionary constraints on the X-ray luminosity function and the luminosity–temperature correlation to determine the best-fitting model parameters.

1 INTRODUCTION

A precise determination of the evolution of X-ray properties of clusters of galaxies will shortly be available. In particular, the X-ray luminosity function (XLF) and the luminosity–temperature (L–T) correlation are open to accurate measurement through, in the first case, serendipitous imaging surveys and, in the second, targeted spectral observations of known X-ray clusters. The aim of this paper is to develop a theoretical framework within which these data may be placed.

The first predictions for the evolution of cluster X-ray properties (eg., Kaiser, 1986) were based on the assumption of self-similar evolution of both the cluster gravitational potential and the intra-cluster medium (ICM). Relatively few conditions need to be met in order for the evolution of the dark-matter component to satisfy this type of evolution. As such, these models are more generally applicable than those that attempt to determine the distribution of cluster masses explicitly (eg., Press & Schechter, 1978). However, whereas the Press-Schechter scheme can be used to predict the distribution — and even conditional distributions — of cluster properties, the self-similar model provides only a scaling of cluster properties between epochs.

For realistic primordial density fluctuation spectra, application of the self-similar assumption to both cluster components predicts that the XLF evolution is strongly positive (ie., an increasing number of X-ray luminous clusters with increasing redshift or look-back time). This has, however, proved contradictory to the observational evidence: the present debate centres on whether the X-ray luminosity function is non-evolving or whether it falls with redshift (eg., Edge et al., 1990, Henry et al., 1992, Rosati et al., 1995, Castander et al., 1995, Nichol et al., 1996).

In order to solve this problem, Kaiser (1991) and Evrard & Henry (1991, EH) proposed that the ICM was initially hot even before falling into the cluster. The early heating of the

gas gives it an initial entropy. Shock heating during cluster collapse may increase the present-epoch entropy above this value, but cannot decrease it. A fall in the entropy can only be achieved by radiative cooling of the gas — this occurs by recombination or Bremsstrahlung radiation, or through inverse Compton scattering of microwave background photons (cf., Padmanabhan, 1995). If the initial heat input occurs at low enough redshift, these processes are inefficient outside virialised regions, and the gas retains a memory of its initial entropy as it clumps together to form larger and larger mass units. Thus the ICM is imprinted with a minimum entropy and hence a maximum density to which the core gas can be compressed without greatly increasing the central temperature and pressure. The papers referenced above showed that the evolution of the XLF was modified in the desired sense. However, this particular physical scenario creates only a single model. With steadily improving observations of distant clusters, it is becoming possible to test between a whole family of models that span these extremes, and even go beyond. EH suggest the general form $L_x \propto (1+z)^s M^p$, but only briefly explore the physical significance of their parameters s and p .

In this paper, I present a more flexible scheme for including the effects of entropy. The new approach has the advantage that the evolutionary parameters may be directly interpreted in terms of the physical processes heating, pre-heating and cooling the ICM. Focusing the discussion on the evolution of entropy automatically separates the contributions of the gravitational evolution of the cluster (which results in adiabatic compression of the ICM) and the specifically gas-phase phenomena, such as shock heating and radiative cooling, which alter the adiabat on which the gas lies. The model thus parameterises the evolution of clusters in such a way as to provide a continuum spanning between the self-similar model and the constant entropy model of EH. It naturally generalises to include the case where the entropy of the central gas declines during the lifetime of the cluster, as

is the case if the radiative cooling of the ICM dominates over the shock heating that occurs during cluster-cluster mergers.

The structure of the paper is as follows. Section 2 develops the entropy-driven model, firstly by introducing the concept of cluster-core entropy and then by parameterising its evolution through the parameter ϵ . The physical processes affecting the core entropy are discussed in Section 2.2, and revised scaling relations are discussed in Sections 2.3 and 2.4. Finally, in Section 2.5, I describe a limitation to the viability of the evolutionary model. Section 3 discusses the role of radiative cooling in the evolution of the ICM, including a comparison with the cooling-flow driven model of Waxman & Miralda-Escude (1995) in Section 3.2. In Section 4, I consider the practical problem of using realistic observational data to constrain the allowed range of evolutionary models. Although the currently available data for distant clusters are relatively poor, significant restrictions are already imposed. Furthermore, it is clear that the definition of a unique model will be feasible in the near future. A summary of the conclusions of this paper is presented in Section 5.

Throughout this paper, I assume that the growth and collapse of cluster-scale density perturbations occurs in a critical density universe. In such a universe, the gravitational growth of clusters is described by the effective slope of the density fluctuation power spectrum (n), and it is sufficient to introduce a single parameter (ϵ) to describe the evolution of the minimum entropy of the intra-cluster medium. This restriction ensures that the scaling relations on which I draw can be robustly justified, and ensures that the model parameter-space is suitably limited. However, by suitable reformulation of the growth of cluster properties, it is possible to generalise these results to the evolution of clusters in an open or vacuum-energy dominated universe. This work will be presented in a subsequent paper.

2 A FAMILY OF ENTROPY-DRIVEN EVOLUTIONARY MODELS

2.1 Why introduce Entropy?

As described by EH, the gas core radius, r_c , the cluster virial radius, r_v , the central gas density, ρ_c , and the mean background density, ρ_b , are related through

$$\left(\frac{r_c}{r_v}\right)^3 \sim \left(\frac{\rho_c}{\rho_b}\right)^{-1/\beta} \quad (1)$$

where β is the standard density profile parameter: $\rho(r) = \rho_c (1 + (r/r_c)^2)^{-3\beta/2}$. This expression assumes that the gas density at the virial radius is a constant multiple of the background density, and that the gas density profile traces the total mass density profile in the outer parts of the cluster but flattens out within $r < r_c$ to form a core. This core is assumed to be present only in the gas distribution: the mass is assumed to maintain its $r^{-3\beta}$ slope to much smaller radii. Clearly, an equivalent of Equation 1 could also be derived for other density profile parameterisations such as that proposed by Navarro, Frenk & White (1995, NFW). Since this profile is no longer a simple power-law, it would greatly complicate the form of the equations that follow. However, in order to model the evolution of clusters over a limited range of redshift, it is adequate to approximate the density

profile by its local gradient (ie., $\beta \approx -\frac{1}{3} \frac{d \ln \rho}{d \ln r}$).

In order to elucidate the physical significance of the gas core, it is necessary to introduce the concept of specific entropy. This is defined as

$$s = c_v \ln \left(\frac{T}{\rho^{\gamma-1}} \right) \quad (2)$$

where T is the gas temperature, c_v is the specific heat capacity of the gas at constant volume and γ is the ratio of specific heats at constant pressure and constant volume. Since the temperature profile of the gas remains approximately flat outside the cluster core, s must fall towards the cluster centre. Note that even though recent ASCA results have shown that the temperature profile is not exactly constant (eg., Markevitch et al., 1996, Markevitch, 1996), this statement remains true because of the very strong radial dependence of the gas density. For example, the gas density falls by a factor 300 over the range of Markevitch et al.'s temperature measurements: if the gas were to have no radial entropy gradient, this would imply a factor of 50 change in temperature over this range. The observed factor is 3. The core in the gas distribution corresponds to a minimum in the gas entropy:

$$\rho_c \approx (T e^{-s_{\min}/c_v})^{1/(\gamma-1)} \quad (3)$$

In what follows, I will take the view that the core in the density distribution *is caused by* the existence of a minimum entropy of the ICM (an alternative interpretation is briefly discussed in Section 3.2). Writing Equation 3 in terms of entropy and temperature therefore separates the effects of adiabatic compression (increases T , but leaves s_{\min} unchanged), and shock heating and/or radiative cooling (increases [or reduces] s_{\min} with little effect on T). The last part of this statement follows from the assertion that the global cluster temperature is proportional to the cluster virial temperature and the assumption that the cluster is roughly isothermal outside the cluster core.

A more detailed understanding of the balance between gas entropy and temperature (or pressure) is clearly desirable. However, although spherically symmetric infall models (eg., Bertschinger, 1985) can give some insight into the build-up of gas in the cluster potential, they are inherently unrealistic since the growth of clusters is intrinsically hierarchical. Reliable progress can only be made through high resolution hydrodynamic simulations, such as those presented by NFW; but these must be analysed with caution to ensure that the finite resolution is fully taken into account. By focusing attention on the entropy of the gas only in the core of the cluster, much of the complexity of this issue can be side-stepped. In what follows, I treat the evolution of the core gas entropy as a phenomenon that is to be determined empirically.

So far, however, I have achieved little practical advance. EH developed this model by assuming that s_{\min} was non-evolving. Advances in the measurement of the X-ray evolution of clusters now justify a more general set of models. This paper expands EH's work by parameterising the evolution of the central gas entropy as a power of the expansion factor:

$$s_{\min} = s_{\min}(z=0) + c_v \epsilon \ln(1+z). \quad (4)$$

Each value of the parameter ϵ generates a new model for the

evolution of the X-ray properties of galaxy clusters which can be interpreted in terms of the physical processes responsible for the heating and cooling of the intra-cluster gas. With this parameterisation of the core gas entropy, the evolution of the relative density of gas in the core can be written

$$\frac{\rho_c}{\rho_b} \propto T^{\frac{1}{\gamma-1}} (1+z)^{-3-\frac{\epsilon}{\gamma-1}}. \quad (5)$$

Equivalent expressions can be derived for other density profile slopes. The main effect of altering the beta parameter is to change the redshift dependence implied by a given ϵ . Since, as I will argue in Section 4, the value of epsilon must be determined from the data itself, a consistent description of the cluster evolution will be obtained even if the true value of β differs slightly from the value assumed. In the discussion that follows, I fix β at its fiducial value of 2/3. This provides a coherent treatment within which cluster evolution can be discussed.

2.2 The Physical Significance of the ϵ Parameter

There are three important regimes for the entropy evolution parameter. This section briefly outlines their physical interpretation.

The case $\epsilon < 0$ corresponds to an intra-cluster medium that is being continually heated in each generation of cluster collapse. This may arise purely due to the action of shock waves during the cluster relaxation process, but the injection of heat by the galaxies themselves (for example, in the form of supernova blast waves) may also contribute. It is extremely difficult to estimate the heating rate *ab initio*, even if shock heating is considered alone. The simulations of NFW suggest that most of the energy in the shock front is deposited in the outer-parts of the cluster; the shocks reaching the central part becoming weak. This suggests that we should expect values of ϵ close to zero. It is, however, possible that more negative values might be found in real clusters due to the cumulative effect of large numbers of weak shocks that are not well-resolved in the simulations.

One particular negative value of ϵ corresponds to the case in which the evolution of the cluster's ICM parallels the evolution of its dark matter potential. This is the familiar self-similar evolution model introduced by Kaiser (1986). The value of entropy evolution parameter required to produce self-similarity (ie., $\frac{\rho_c}{\rho_b}$ constant) depends on the spectrum of density fluctuations and the ratio of specific-heats. Assuming $\gamma = 5/3$, as appropriate for a monatomic gas,

$$\epsilon_{SS} = -\left(\frac{n+7}{n+3}\right) \quad (6)$$

where n is the effective spectral index of density fluctuations on cluster scales (ie., $\delta\rho_b/\rho_b \propto r^{-(n+3)/2}$). For flatter power spectra, each successive scale collapses in rapid succession and the heating of the ICM must become stronger if self-similarity is to be maintained. For example, $n = -1$ requires $\epsilon_{SS} = -3$; $n = -2$ requires $\epsilon_{SS} = -5$.

As I have already described, the constant entropy model of EH corresponds to $\epsilon = 0$. This model is appropriate if the shocks that are generated during the growth of clusters are ineffective at heating the gas in the core of the cluster. In this model, it is possible to interpret s_{\min} as a 'primordial' entropy that was established in the gas before it became

bound into clusters.

In the set of models with $\epsilon > 0$, the gas in the core of the cluster is able to radiate a significant fraction of its internal energy over the Hubble time. This radiation gives rise to the 'cooling flows' that are well established in nearby clusters (eg., Fabian et al., 1991), and have recently been detected also in distant systems (eg., Donahue & Stocke, 1995). The likely contribution of radiative cooling to ϵ is discussed in Section 3.

2.3 The Connection with Cluster X-ray Luminosity

EH show that the X-ray luminosity of a cluster is

$$L_X \propto T^\alpha \rho_c^2 r_c^3 \quad (7)$$

where the appropriate value of the exponent α depends on whether the luminosity is measured with a bolometric or wide-band detector ($\alpha \sim 1/2$) or through a low-energy band-pass ($\alpha \sim 0$) as would be appropriate for the ROSAT or Einstein satellites. Using Equation 1, the X-ray luminosity can be written in terms of the background density (ρ_b , which is set by the cosmic epoch), the cluster's total mass (M) and virial temperature (both of which are properties of the dark-matter component of the cluster), and the ratio of the cluster core density to the background density (this is determined by the entropy of the central gas):

$$L_X \propto \rho_b T^\alpha M \left(\frac{\rho_c}{\rho_b}\right)^{2-(1/\beta)} \quad (8)$$

Combining this with the evolution of the gas core density described by Equation 5, and relating the cluster temperature to mass through $M \propto T^{3/2} (1+z)^{-3/2}$ gives

$$L_X \propto (1+z)^{3/2-(3+\frac{\epsilon}{\gamma-1})(2-\frac{1}{\beta})} T^{\alpha+3/2+(\frac{1}{\gamma-1})(2-\frac{1}{\beta})} \quad (9)$$

The appearance of this relation is substantially improved by setting $\gamma = 5/3$ and restricting attention to cluster profiles with $\beta = 2/3$:

$$L_X \propto (1+z)^{-3\epsilon/4} T^{(9/4)+\alpha} \quad (10)$$

2.4 Strong versus Weak Self-Similarity

So far, I have not needed to be careful about the exact meanings of the terms used in (eg.) Equation 10. In principle, T , L_X , M etc., apply to individual clusters, but it is by no means clear that the constant of proportionality that links them should be the same for all clusters. For instance, studies of the growth of hierarchical clusters (eg., Lacey & Cole, 1993) show that a great variety of trajectories may lead to an individual cluster of given mass at the present epoch. To give an explicit example, we should more correctly interpret the redshift (z), appearing in Equation 10, as the epoch at which the cluster last had a major merger event rather than the epoch at which the cluster is observed (cf., Kitayama & Suto, 1996).

The Weak Self-Similarity principle (eg., Kaiser, 1986) asserts that, although there is considerable scatter between the formation histories of individual clusters, relations of the form of Equation 10 can be used to relate the characteristic properties of cluster populations at one cosmic epoch to

those at another. The reasoning behind this is that — so long as the power spectrum of density fluctuations contains no additional scale — the only physical scale that distinguishes the properties of clusters at one epoch from those at another is the scale at which average density fluctuations make the transition between linear and non-linear growth. In order that Equation 10 then fits into this scheme, we must be careful also to interpret Equation 4 as applying to the characteristic central entropy of the cluster population (where we may either consider the cluster population as a whole, or limit ourselves to a well-defined relative sub-population such as the most massive 10% of the population).

The form of Equation 10 has been chosen to separate the evolution of the clusters' X-ray luminosity that comes from the increasing characteristic density of the universe, and the component that comes from the changing characteristic temperatures of clusters. Adopting a particular form for the slope of the density fluctuation power spectrum, I arrive at the scaling relation

$$\frac{\Delta \log L_X}{\Delta \log(1+z)} = \left(\alpha \left(\frac{n-1}{n+3} \right) + \frac{9-3\epsilon}{4} - \frac{9}{n+3} \right). \quad (11)$$

This illustrates the balance of terms tending to increase and decrease the luminosity as a function of redshift. Flatter power spectra (more negative n) and more positive entropy evolution both tend to reduce the X-ray luminosities of distant clusters. This is balanced by an intrinsic increase in the efficiency of X-ray emission due to the high average density of the universe. Figure 1 illustrates this interplay between the power spectrum and entropy evolution by applying the scaling of Equation 11 to the low-redshift luminosity function of Edge et al., 1990. More precise definition of the local luminosity function will shortly be available from the ROSAT All-Sky Survey (eg., Ebeling et al., 1996); however, because of the degeneracy seen in this figure, it is difficult to interpret the evolution of the X-ray luminosity function in terms of a single combination of n and ϵ . The two effects become easier to discriminate, however, as a greater range of X-ray luminosities is probed (cf., Castander et al., 1995).

Writing Equation 10 to separate the effects of redshift and temperature tempts another approach. The form of the relation appears to suggest that the slope of the present-day L_X - T correlation should be $\alpha + 9/4$. As noted by Evrard & Henry, this is encouragingly close to the observed L_X - T slope ($L_X^{\text{bol}} \propto T^3$, eg., Edge & Stewart, 1991, David et al., 1994). However, this prediction goes far beyond the weak self-similarity principle that I have described above: it requires that I apply the scalings not to the characteristic properties of the clusters at a particular epoch, but to interrelate the properties of clusters at the same epoch. This is the so-called Strong Self-Similarity Principle. For the reasons I have described above, in particular the different average formation histories of high and low-mass clusters, it has little physical basis. To illustrate this point, the slope of the L_X - T appears to be in 'agreement' with the observations even if $\epsilon = \epsilon_{SS}$ (Equation 6). This contrasts with the standard self-similar model (eg., Kaiser, 1986) that 'predicts' $L_X \propto T^{(3/2)+\alpha}$ at a fixed epoch. The discrepancy is not real, and has arisen because the Strong Self-Similarity Principle requires that s_{min} in Equation 4 applies to all clusters regardless of their mass, rather than to the characteristic entropy of the cluster population. This is an additional as-

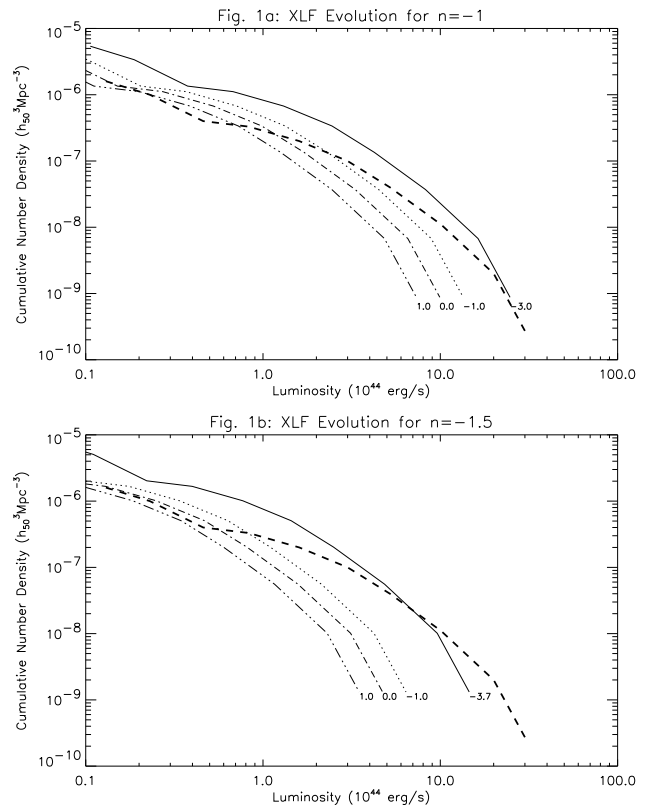


Figure 1a, b. The evolution of the X-ray luminosity function. The dashed line shows the present-day cumulative X-ray luminosity function of Edge et al., 1990. The evolution of the gravitational potential is described by self-similar evolution with power spectra of -1 (panel a) and -1.5 (panel b). The solid lines show the $z = 0.5$ luminosity function predicted for self-similar evolution of the ICM ($\epsilon = \epsilon_{SS}$, Equation 6); milder heating of the ICM, $\epsilon = -1$, is shown by the dotted line; dot-dashed lines show the luminosity evolution for constant core entropy, $\epsilon = 0$; and dot-dot-dashed lines illustrate a model in which gas cooling dominates the entropy evolution, $\epsilon = +1$. All three calculations use $\alpha = 0.5$ and $\beta = 2/3$.

sumption for which there is no prior physical justification.

Although Equation 9 cannot therefore be used to estimate the slope of the present-day L_X - T correlation robustly, it does predict how the normalisation of the correlation will evolve. Because the slope of the observed relation is close to the temperature dependence of Equation 10, the evolution of this relation is dominated by ϵ (Figure 2). This breaks the degeneracy between ϵ and n inherent in luminosity function measurements. Thus, by combining the measurement of both the L_X - T correlation and the luminosity function at high redshift, the separate roles of the power-spectrum and the core gas entropy can be distinguished without having to measure the evolution of the temperature function directly. The practical feasibility of this approach is discussed in Section 4.

2.5 Limit on the Validity of the Model

The model that I have described implicitly assumes that the core radius is set by the minimum entropy of the cluster gas remains well inside the cluster's virial radius. This corresponds to the standard picture of a cluster in which the gas

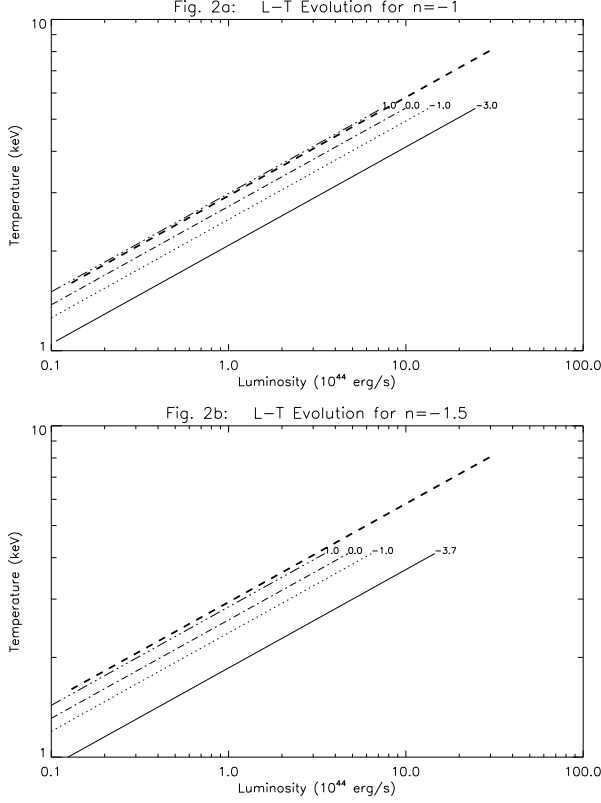


Figure 2a, b. The predicted evolution of the X-ray luminosity – temperature correlation. Panel a shows $n = -1$; panel b, $n = -1.5$. The thick dashed line shows the position of the present-day correlation from David et al., 1993 (as appropriate for bolometric luminosities). The other line types illustrate the effect of different choices of the ϵ parameter on the correlation at $z = 0.5$. The evolution of the correlation is only weakly affected by the choice of density fluctuation spectral index, n . This most strongly affects the range of cluster temperatures that will be observed. As in Figure 1, I have used $\alpha = 0.5$ and $\beta = 2/3$.

is confined by a virialised dark matter halo.

The scaling of the ratio of the core and virial radii is given by

$$\frac{\Delta \log \left(\frac{r_c}{r_v} \right)}{\Delta \log(1+z)} = \frac{1}{3\beta(\gamma-1)} \left[3(\gamma-1) + \epsilon - \left(\frac{n-1}{n+3} \right) \right] \quad (12)$$

Adopting a typical present-day ratio of 1/10 for r_c/r_v , and setting β and γ to their standard values, the epoch at which the gas is no longer trapped within the virial radius of a typical halo is

$$\log(1+z_{\max}) = \left[\frac{3}{4} \left(\epsilon + \frac{n+7}{n+3} \right) \right]^{-1} \quad (13)$$

This limit becomes more problematic for larger values of ϵ and flatter (more negative) power spectra. For example, $(n, \epsilon) = (-1, +1)$ has $z_{\max} = 1.2$ while $(n, \epsilon) = (-2, +1)$ has $z_{\max} = 0.67$. Even in these cases, however, the model still provides a framework for understanding the evolution of galaxy clusters over the range of redshifts that are currently observable. Furthermore, when $r_c \sim r_v$, the scaling relations may continue to apply if the cluster's gravitational potential is sufficiently smooth and well-defined in the infall region.

3 THE ROLE OF RADIATIVE COOLING IN CLUSTER EVOLUTION

3.1 Estimating the Evolution of Gas Entropy due to Cooling

During cluster mergers, dissipation of the bulk motion of the gas tends to raise the specific entropy of the ICM. Although it is difficult to estimate the effectiveness of this process for core gas, it is clear that we should expect $\epsilon < 0$. The radiative cooling of the intra-cluster gas, which occurs principally at X-ray wavelengths, acts in the opposite sense. In this section, I use the observed temperatures and densities of gas in the cores of present-day clusters to estimate an effective value for ϵ_{cool} , the radiative cooling contribution to the ϵ parameter. In the absence of alternative cooling mechanisms, this estimate is an upper limit to the value of ϵ that will actually occur.

The change in specific entropy with time due to radiative cooling is given by

$$\frac{ds}{dt} = - \frac{K_L n_e}{T \mu_H m_H} \quad (14)$$

where K_L is the cooling coefficient (ie., the radiated power per unit volume is $K_L n_e n_H$), n_e is the electron number density, μ_H is the relative atomic mass of the plasma per hydrogen atom, m_H is the atomic mass unit, and T is the gas temperature in Kelvin. For a cosmic abundance plasma with temperature $\sim 5 \times 10^7$ K, eqn. 14 can be written

$$\frac{ds}{dt} = -1.8 \times 10^{-10} \left[\frac{n_e}{10^{-3} \text{ cm}^{-3}} \right] \left[\frac{K_L}{2 \times 10^{-23} \text{ erg s}^{-1} \text{ cm}^3} \right] \times \left[\frac{T}{5 \times 10^7 \text{ K}} \right]^{-1} \text{ erg s}^{-1} \text{ K}^{-1} \text{ g}^{-1} \quad (15)$$

For such a plasma, the specific heat capacity is

$$c_v = \frac{\frac{3}{2} k_B}{\mu m_H} = 2.07 \times 10^8 \text{ erg K}^{-1} \text{ g}^{-1} \quad (16)$$

where μ is the mean molecular weight per free particle. Using the definition of ϵ given in Equation 4, and transforming Equation 14 to a derivative with respect to $1+z$, the effective value of the dimensionless entropy parameter can be expressed as:

$$\epsilon_{\text{cool}} = 0.53 (1+z)^{-3/2} h_{50}^{-1} \left[\frac{n_e}{10^{-3} \text{ cm}^{-3}} \right] \times \left[\frac{K_L}{2 \times 10^{-23} \text{ erg s}^{-1} \text{ cm}^3} \right] \left[\frac{T}{5 \times 10^7 \text{ K}} \right]^{-1} \quad (17)$$

where the Hubble constant is parameterised by $H_0 = 50 h_{50} \text{ km s}^{-1} \text{ Mpc}^{-1}$.

The redshift dependence of ϵ_{cool} can be estimated by combining Equations 5 and 7. Adopting $\gamma = 5/3$, ϵ_{cool} varies as $(1+z)^{-3(1+\epsilon)/2} T^{1/2}$, so that even if the low redshift evolution is dominated by cooling, it becomes less and less important as we look to higher redshifts.

By extracting from the literature values for T and n_e for gas in the centres of present-day clusters of galaxies, it is possible to estimate the appropriate values of ϵ for specific systems. These will serve as a guide to the value of ϵ that applies to the cluster population of as a whole. For the Coma cluster (Briel et al., 1991), I find $\epsilon_{\text{cool}} = 0.80$; for the extreme cluster A2163, $\epsilon_{\text{cool}} = 1.5$ (Markevitch et al., 1996)

[both calculations assume $h_{50} = 1$]. As I have stressed, the actual value of ϵ that describes the X-ray evolution of galaxy clusters is likely to be less than ϵ_{cool} due to the heating of core gas during cluster formation. However, the analysis of this section shows that we can conservatively expect that $\epsilon < 2$ at the present-day, with the limit becoming even more stringent at higher redshifts. This sets an important upper limit of the strength of the decline in the X-ray luminosities of clusters.

3.2 Comparison with the Cooling Flow-Driven Model of Waxman & Miralda-Escude

Waxman & Miralda-Escude (1995, WM-E) present a model for the evolution of spherical clusters in which the core in the gas density profile is set by the surface (the ‘cooling radius’) at which the cooling time of the gas equals the age of the universe at the epoch under consideration. The evolution of the gas core density with redshift is thus set by the competition between the increasing cooling efficiency (due to higher characteristic densities) and the falling age of the universe. For a $\beta = 2/3$ cluster profile, they find

$$\frac{\rho_c}{\rho_b} \propto T^{1-\alpha'} (1+z)^{-3/2} \quad (18)$$

where $\alpha' \approx 1/2$ parameterises the temperature dependence of the *bolometric* X-ray luminosity (as opposed to the luminosity measured by a band-pass detector). Comparison with Equation 5 shows that the cooling flow model can be formally incorporated into the entropy-driven model by setting $\gamma = 1 + 1/(1 - \alpha') \approx 3$ and $\epsilon = -3/2(1 - \alpha') \approx -3$. The value of γ required does not, however, have a physical interpretation: the temperature dependence of the density ratio is considerably weaker than in the standard $\gamma = 5/3$ entropy-driven model.

The evolution of X-ray luminosity in WM-E’s model is given by

$$L_X \propto T^{2+\alpha-(\alpha'/2)} (1+z)^{3/4}. \quad (19)$$

Comparing this with Equation 10 shows that, compared to an $\epsilon > -1$ entropy driven model, the cooling flow model will produce more rapid increase (with redshift) in X-ray luminosity at a given temperature. Although in both cases the ratio of the gas core radius to the virial radius increases with redshift, at a given temperature, the strength of this effect is larger for the $\epsilon > -1$ model. Thus in the latter class of model, an ever smaller fraction of the ICM becomes susceptible to the cooling flow instability. Fortunately, observation of the evolution of the L_X - T correlation will provide a simple test by which the two classes of model can be distinguished. Only the entropy-driven model is able to account for a relation that is non-evolving or in which the X-ray luminosity at a given temperature falls with redshift.

Although WM-E’s cooling flow driven model cannot naturally be expressed in terms of a particular value of ϵ , the general nature of the models presented here guarantees that the observational signature of such models can be reproduced by an apparent combination of n and ϵ parameters. I describe the parameters as ‘apparent’ since although they reproduce the observations, they will not correspond to true spectral index, or describe the true evolution of cluster central entropy. Comparing equations 19 and 10 shows

that relation between the true and apparent spectral index is given by $\frac{n_{\text{app}}-1}{n_{\text{app}}+3} = \frac{7}{9} \left(\frac{n-1}{n+3} \right)$ (for example, a true spectral index of -1.0 would give an apparent index of -0.75) and that all WM-E models will have $\epsilon_{\text{app}} = -1$. In the following section, I will examine how realistic data may be used to constrain the true cluster evolution model in (n, ϵ) parameter space. It must, however, be clearly stated that a measurement of $\epsilon \approx -1$ may be equally well interpreted within the entropy-driven model described in this paper, or within the cooling-flow driven model described by WM-E.

4 OBSERVATIONAL CONSTRAINTS ON THE PARAMETERS N AND ϵ

Measurement of the evolution of the galaxy cluster temperature function would provide a clean test of the rate of cluster mass growth and thus allow accurate determination of the density fluctuation spectral index effective on cluster scales (eg., Eke et al., 1996). An idealised measurement would be made from a cluster survey in which selection was based on temperature and was independent of cluster X-ray flux or luminosity. In practice, such a survey would have to be constructed from a flux limited cluster sample. One strategy would be to discard enough clusters to create a volume limited subsample, to measure the temperatures of these clusters and then to apply a second threshold so that the sample became complete in temperature. A clearly preferable procedure would use two data-sets to define separately the evolution of the X-ray luminosity function (XLF) and the evolution of the X-ray luminosity – temperature (L- T) correlation. Within the entropy-driven model, these two pieces of data create near-orthogonal constraints on the parameters n and ϵ thus allowing us to piece together the complete picture of cluster evolution. While the two data-sets must refer to clusters of similar luminosities, there is no requirement that the L- T correlation be determined from a statistically complete sample.

Figure 3 illustrates the constraint that can be placed on the values of n and ϵ for a range of hypothetical evolutionary measurements. Throughout this section, I have assumed that the density profile can be adequately approximated by setting $\beta = 2/3$. Solid lines illustrate the constraint from the evolution of the XLF. The figure assumes that the cumulative XLF can be approximated by a power-law of slope -1.2 over the relevant range of X-ray luminosities and sets $\alpha = 0$, as appropriate for a low energy band-pass detector such as ROSAT. The lines are labeled by the logarithm of change in the XLF amplitude (measured at a fixed X-ray luminosity) between the present-day and $z = 0.5$. For example, the line labeled 0 shows the constraint implied by a non-evolving luminosity function; that labeled by -0.3 is the constraint implied by a factor of 2 fall in XLF amplitude. Dashed lines in the figure show the equivalent constraint implied by a measurement of the evolution of the L- T correlation. The labels give the logarithm of the change in the normalisation (ie., temperature at a fixed X-ray luminosity) between the present-day and $z = 0.5$. An L- T inverse slope of 0.30 is assumed, and the luminosities are taken to be bolometric (ie., $\alpha = 0.5$).

Any single evolutionary measurement (of either the XLF or the L- T correlation) can be reproduced by a wide

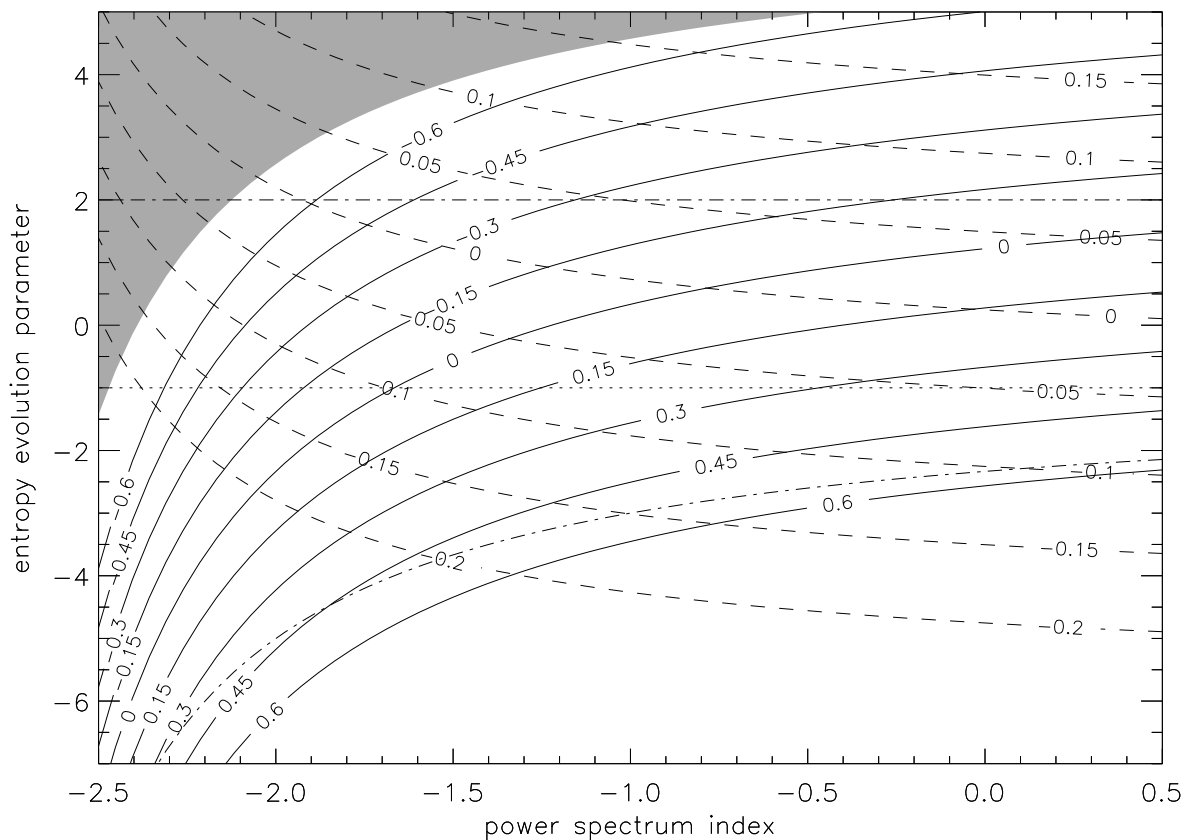


Figure 3. Constraints on the parameters n and ϵ inferred from the evolution of the X-ray luminosity function (solid lines) and the evolution of the luminosity – temperature relation (dashed lines) as it might be measured at redshift 0.5. The lines are labeled by the logarithm of the change in normalisation: further details are given in the text of Section 4. Dot-dashed lines indicate values of the ϵ parameter corresponding to self-similar evolution (bottom line) and evolution dominated by radiative cooling (upper line); while the dotted line shows parameter space occupied by the cooling-flow driven models of WM-E. The shaded area indicates the region of parameter space in which the underlying assumptions of our model are no longer valid at redshift 0.5.

range of (ϵ, n) parameter pairs. However, measurement of the evolution of both observable relations removes this degeneracy. For flat power spectra (ie., more negative n), the lines of given XLF and L-T evolution are nearly orthogonal. Thus in this region even low accuracy measurements can place stringent constraints on n and ϵ . As n becomes more positive, the rate of gravitational growth slows down and the evolution of both the XLF and L-T relations is driven by entropy evolution alone. In this region of the diagram, the two measurements become more degenerate and greater accuracy is required to determine n .

The figure also gives two dot-dashed lines illustrating the limiting physical models. The lower line shows the curve defined by self-similar models, $\epsilon = \epsilon_{SS}$. Unless gas is heated more than the dark matter during cluster collapse, the evolutionary model must lie above this line. The upper line shows the maximum evolution due to radiative cooling ($\epsilon = 2$) suggested by the analysis of Section 3. Unless some other cooling mechanism can be invoked, or the value of β is significantly different from $2/3$, an acceptable model must lie below this line. In addition, the shaded upper left-hand corner illustrates the area of parameter space for which z_{\max} (as defined by Equation 13) is less than 0.5. The underlying

assumptions of the model are no longer valid in this region. The shaded region would become larger if we were to trace the evolution to still higher redshifts. Finally, I have added a dotted line to the figure to show the area of (apparent) parameter space occupied by the models of WM-E.

Although current data leave the evolution of the XLF and the L-T correlation poorly defined, it is already interesting to investigate the limits that are implied. The situation is shown in Figure 4, where solid lines show the constraint from luminosity function measurements. Dashed lines show the constraints from the temperature function. The comparison is made at a nominal luminosity of $10^{44} \text{ erg s}^{-1}$. To define the lower limit to evolution of the XLF, I take the recent reanalysis of the EMSS survey by Nichol et al., 1996. Using deeper ROSAT images of a number of the EMSS clusters, they conclude that a non-evolving XLF cannot yet be excluded. This forms the lower solid line. The upper line shows a 40% fall in XLF amplitude as suggested by Castander et al., 1995, from the analysis of serendipitous ROSAT fields. Both measurements are taken to have a median redshift of 0.35 and have been normalised using the low redshift luminosity function of Henry et al. (1992). Data for the evolution of the L-T relation are taken from Tsuru et al., 1996 (and

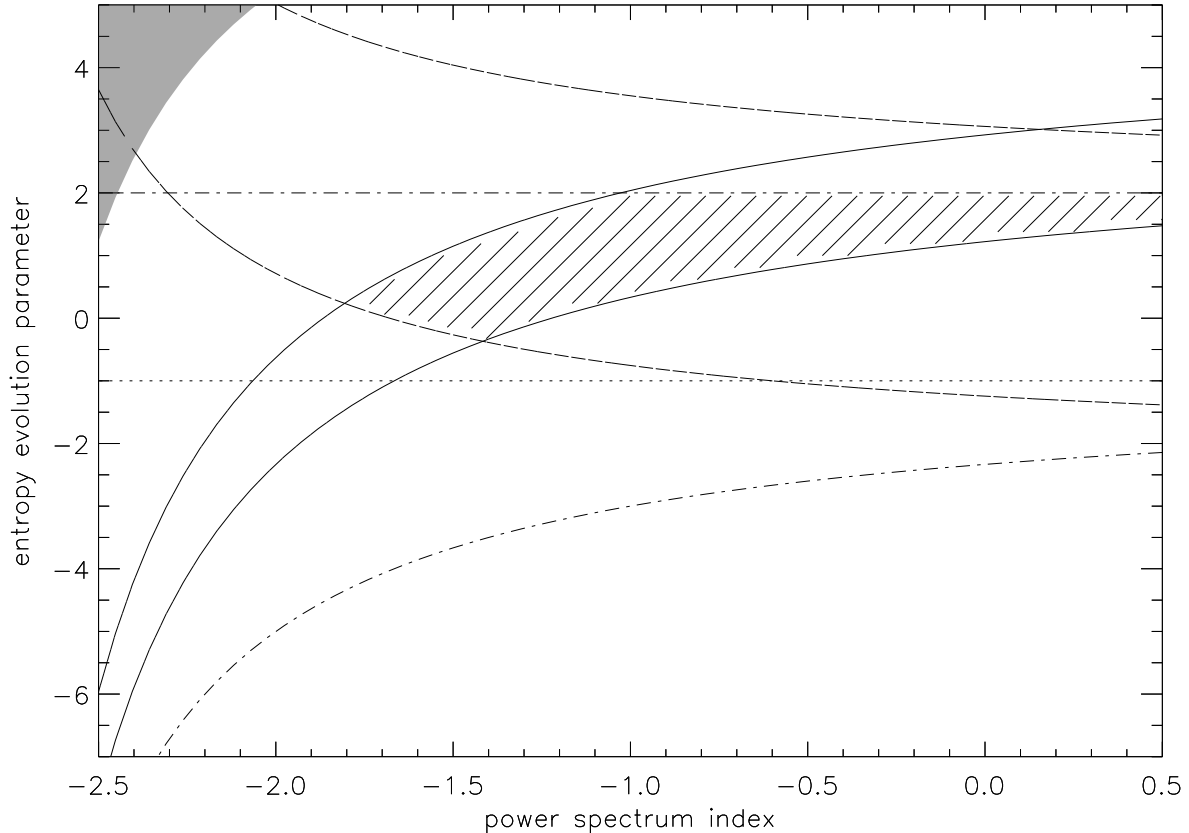


Figure 4. Preliminary constraints on the cluster evolutionary model from current data for distant clusters. Solid lines show the present limits of the X-ray luminosity function evolution at $\bar{z} = 0.35$ from Castander et al., 1995 (upper line), and Nichol et al., 1996 (lower line). Dashed lines illustrate the formal 90% confidence limits derived from the $\bar{z} = 0.21$ luminosity–temperature correlation of preliminary ASCA data (Tsuru et al., 1996). Acceptable models (indicated by the hashed region) must lie between these lines and below the limit $\epsilon < 2$. The evolutionary calculations assume $\alpha = 0.0$ for the luminosity function data and $\alpha = 0.5$ for the luminosity–temperature correlation data. Dotted and dot-dashed lines are carried over from Figure 3; the shaded corner of the plot indicates the area of parameter space in which the evolutionary model is invalid at $z = 0.35$.

normalised using $z < 0.1$ data from David et al., 1993). It should be noted that Tsuru et al.’s results are based on *preliminary* reduction of data from the ASCA satellite and should therefore be treated with caution. Furthermore, the data have a median redshift of only 0.21, so the evolutionary constraint that can be derived from their data has relatively little leverage. The two curves show a change in logarithmic normalisation of between -0.028 and $+0.053$ (ie., an uncertainty of $\pm 10\%$ in the distant cluster L–T correlation amplitude), corresponding to the 90% formal confidence limits of Tsuru et al.’s data.

A cursory inspection of the figure is disappointing: the density fluctuation index n can have any value greater than -1.7 . Yet even these data make a number of points clear. Firstly the data are inconsistent with any very flat spectral index. While values of n around -2 are able to reproduce the observed XLF evolution, they produce too much evolution in the L–T relation to be acceptable. It is clear that none of the self-similar models can account for the observed evolution; but the data suggest that the combined XLF and L–T data permit only models in which gas cooling dominates over heating. Furthermore, although these preliminary data

provide only a weak constraint on the spectral index, the figure shows that even a modest improvement in the accuracy of the distant cluster L–T relation, or the median redshift at which it can be determined, will considerably refine the determination of n .

5 CONCLUSIONS

The basic aim of this paper has been to produce a general framework describing the evolution of the X-ray properties of galaxy clusters. In contrast to previous work, the model I have presented explicitly differentiates between the contribution from the evolution of the gravitational potential, and the component due to the evolution of the entropy of the cluster core gas. This division of the evolution into two components ensures that each realisation of the model then has a physical interpretation: the evolution of the gravitational component is derived from the density fluctuation power spectrum and the background cosmological model, while the evolution of the core entropy is determined by the balance between the radiative cooling of the intra-cluster medium and its shock heating during cluster-cluster mergers.

In this paper, I have limited attention to the evolution of clusters in a critical density universe dominated by collisionless dark matter and have assumed that the density fluctuation power spectrum can be represented by an effective spectral index n . These two assumptions allow the evolution of the cluster gravitational potential to be described using the self-similar scaling relations of Kaiser (1986). In contrast, the evolution of the gas distribution is determined by the assumption that the gas has a roughly isothermal distribution with temperature proportional to the cluster virial temperature, and with its core radius set by a minimum entropy constraint. The evolution of cluster X-ray properties is then determined, on the one hand, by the evolution of the cluster virial temperature, and on the other, by the evolution of the central entropy. The entropy evolution is specified by the parameter ϵ (Eqn. 4), which I have regarded as a quantity to be fixed by observation.

The parameters n and ϵ generate a two-dimensional continuum of scaling relations that allow the characteristic properties of clusters at one epoch to be transformed to another. Because the effects of changes in these parameters are close to orthogonal, they allow a very general set of evolutionary scenarios to be generated. Furthermore, each point in the n - ϵ plane has a unique physical interpretation. Some regions of the parameter space can be singled out as having particular interest. One such region is the line of models in which the heating of the ICM during the gravitational growth of the cluster maintains a constant ratio between the cluster core and virial radii. This subset of parameters recovers the original self-similar scaling relations proposed by Kaiser (1986). Another notable dividing line is the upper limit on the entropy evolution parameter that can be set from the observed X-ray surface brightnesses of present-day cluster cores. If gas cooling occurs radiatively, ϵ cannot be larger than 2.

The model described here can, however, only be used to derive scaling relations (ie., to use the properties of clusters observed at the present-day to predict the properties of the cluster population at an earlier time). For this reason, I have been careful to avoid discussion of the way in which the central ICM entropy may vary between clusters of differing masses at a single epoch. This question cannot be addressed without introducing further parameters into the model.

In the final section of the paper, I have illustrated how the observed evolution of cluster properties may be used to discriminate between different models. Although knowledge of the evolution of the X-ray luminosity function alone does not provide enough information to determine n or ϵ uniquely, accurate differentiation is possible if the luminosity function is combined with data on the evolution of the luminosity – temperature correlation. For flatter power spectra, (ie., more negative n) the XLF and L-T constraints impose near orthogonal limits in the n - ϵ parameter space. Thus even quite poor measurements result in significant constraints on the physical model (ie., the rate of gravitational growth and rate of gas heating/cooling) underlying cluster evolution. As a result, definition of this model is easily within the scope of current and near-term X-ray missions.

ACKNOWLEDGMENTS

I would like to acknowledge the comments and encouragement of Shaun Cole, Carlos Frenk and Gus Evrard and to thank the anonymous referee for the improvements suggested. This project was carried out using computing facilities supplied by the Starlink Project, and was supported by a PPARC rolling grant for “Extragalactic Astronomy and Cosmology at Durham”.

REFERENCES

- Bertschinger, E., 1985, Ap. J. Suppl., 58, 39
- Briel, U., et al., 1991, A&A, 259, L31
- Castander, F. J., Bower, R. G., Ellis, R. S., Aragon-Salamanca, A., Mason, O., Hasinger, G., McMahon, R. G., Carrera, F. J., Mittaz, J. P. D., Perez-Fournon, I., Lehto, H. J., 1995, Nature, 377, 39
- David, L. P., Slyz, A., Jones, C., Forman, W., Vrtilik, S. D., 1993, ApJ, 412, 479
- Donahue, M., Stocke, J. T., 1995, ApJ, 449, 554
- Ebeling, H., Voges, W., Boehringer, H., Edge, A. C., Huchra, J. P., Briel, U. G., 1996, MNRAS, 281, 799
- Edge, A. C., Stewart, G. C., 1991, MNRAS, 252, 414
- Edge, A. C., Stewart, G. C., Fabian, A. C., Arnaud, K. A., 1990, MNRAS, 258, 177
- Eke, V. R., Cole, S., Frenk, C. S., 1996, preprint
- Evrard, A. E., Henry, J. P., 1991, ApJ, 383, 95 (EH)
- Fabian, A. C., Nulsen, P. E. J., Canizares, C. R., 1991, Astron. & Astrophys. Rev., 2, 191
- Henry J. P., Gioia I. M., Maccacaro T., Morris S. L., Stocke J. T., Wolter A., 1992, ApJ, 386, 408
- Kaiser, N., 1986, MNRAS, 222, 323
- Kaiser, N., 1991, ApJ, 383, 104
- Kitayama, T., Suto, Y., 1996, ApJ, in press
- Lacey, C., Cole, S., 1993, MNRAS, 262, 627
- Markevitch, M., Mushotzky, R., Inque, H., Yamashita, K., Furuzawa, A., Tawara, Y., 1996, ApJ, 456, 437
- Markevitch, M., 1996, ApJ, 465, L1
- Navarro, J. F., Frenk, C. S., White, S. D. M., 1995, MNRAS, 275, 720
- Nichol, R. C., Holden, B. P., Romer, A. K., Ulmer, M. P., Burke, D. J., Collins, C. A., 1996, pre-print.
- Padmanabhan, T., 1993, Structure Formation in the Universe, Cambridge University Press
- Press, W. H., Schechter, P., 1974, ApJ, 187, 425
- Rosati, P., Della Ceca, R., Burg, R., Norman, C., Giacconi, R., 1995, ApJ, 445, 11
- Tsuru, T., Koyama, K., Hughes, J. P., Arimoto, N., Kii, T., Hattori, M., 1996, in *The 11th international colloquium on UV and X-ray spectroscopy of Astrophysical and Laboratory Plasmas* (eds. Watanabe, T., Yamashita, K.) in press
- Waxman, E. & Miralda-Escude, J., 1995, ApJ, 451, 451

This paper has been produced using the Royal Astronomical Society/Blackwell Science \TeX macros.